

Coherent seeding of the dynamics of a spinor Bose-Einstein condensate: from quantum to classical behavior

Bertrand Evrard, An Qu, Jean Dalibard and Fabrice Gerbier

Laboratoire Kastler Brossel, Collège de France, CNRS,

ENS-PSL Research University, Sorbonne Université,

11 Place Marcelin Berthelot, 75005 Paris, France

(Dated: November 27, 2021)

We present experiments revealing the competing effect of quantum fluctuations and of a coherent seed in the dynamics of a spin-1 Bose-Einstein condensate, and discuss the relevance of a mean-field description of our system. We first explore a near-equilibrium situation, where the mean-field equations can be linearized around a fixed point corresponding to all atoms in the same Zeeman state $m = 0$. Preparing the system at this classical fixed point, we observe a reversible dynamics triggered by quantum fluctuations, which cannot be understood within a classical framework. We demonstrate that the classical description becomes accurate provided a coherent seed of a few atoms only is present in the other Zeeman states $m = \pm 1$. In a second regime characterized by a strong non-linearity of the mean-field equations, we observe a collapse dynamics driven by quantum fluctuations. This behavior cannot be accounted for by a classical description and persists for a large range of initial states. We show that all our experimental results can be explained with a semi-classical description (truncated Wigner approximation), using stochastic classical variables to model the quantum noise.

I. INTRODUCTION

The mean-field approximation is an essential tool of many-body physics. In this approach, the interaction of a single body with the rest of the system is treated in an averaged way, neglecting fluctuations around the mean and erasing any spatial correlations. The original many-body problem is then reduced to a much simpler one-body problem, a tremendous simplification enabling a basic analysis of the problem at hand. The accuracy of the averaging improves with the number of particles in direct interaction. Consequently, the mean-field treatment is well suited for highly connected systems, while important deviations are common for systems with short range interactions in reduced dimensions.

When applied to bosonic quantum systems, a mean-field approach often entails another important approximation where intrinsic quantum fluctuations (and the correlations they induce) are neglected. Since quantum fluctuations are reflected in the non-commutativity of observables, field operators in the second-quantization formalism are replaced by commuting c -numbers. A possible improvement consists in replacing the field operators by classical stochastic fields [1–5], with a statistics properly chosen to be as close as possible to the original quantum problem. Such a semi-classical approach allows to account quantitatively for quantum fluctuations, while keeping the inherent simplicity of the mean-field equations.

In this Letter, we study the role of quantum fluctuations and the emergence of mean-field behavior in a quantum spinor Bose-Einstein condensate [6]. The atoms are condensed in the same spatial mode and interact all-to-all. The mean-field approach is thus well appropriate to study the dynamics in the spin sector, and has indeed been successfully used to describe several situations, ei-

ther at [7, 8] or out-of [9–14] equilibrium. More recently, several experiments addressed the dynamics of a condensate prepared in an unstable configuration, achieving a high sensitivity to both classical and quantum fluctuations [15–31].

Here, our goal is twofold. First, we reveal the effect of quantum fluctuations in two different dynamical regimes, corresponding to persistent oscillations or relaxation to a stationary state [31]. Second, we address the relevance of a classical field description by comparing our experimental results systematically with three theoretical approaches. In the fully classical picture (C), we derive mean-field equations of motion and solve them for well-defined initial conditions, possibly including a coherent seed. In the semi-classical picture (SC), we keep the same mean-field equations of motion but for fluctuating initial conditions, with a probability distribution designed to model the quantum noise of the initial state. Finally, we perform a fully quantum treatment (Q), consisting in a numerical resolution of the many-body Schrödinger equation.

II. SPINOR BOSE-EINSTEIN CONDENSATES

We work with Bose-Einstein condensates of N spin-1 Sodium atoms in a tight optical trap. Due to the strong confinement, all atoms share the same spatial wave function $\psi(\mathbf{r})$ [32], such that the spin is the only relevant degree of freedom. In this regime, the Hamiltonian describing the spin-spin interaction is (up to an additive constant) [6, 32–34]

$$\hat{H}_{\text{int}} = \frac{U_s}{2N} \sum_{i,j=1}^N \hat{\mathbf{s}}_i \cdot \hat{\mathbf{s}}_j = \frac{U_s}{2N} \hat{\mathbf{S}}^2. \quad (1)$$

Here $\hat{\mathbf{s}}_i$ denotes the spin of atom i , $\hat{\mathbf{S}} = \sum_i \hat{\mathbf{s}}_i$ the total spin, and U_s the spin-spin interaction energy. In the single-mode limit, the spin-spin interaction is given by $U_s = (4\pi\hbar^2 a_s N/M) \int d^3\mathbf{r} |\psi(\mathbf{r})|^4$, where a_s is a spin-dependent scattering length, M is the mass of a Sodium atom, and the spin-independent spatial mode ψ is the lowest energy solution of the time-independent Gross-Pitaevskii equation [35]. Note that since U_s depends on the atom number N , technical fluctuations in the experiment (*e.g.* of the total atom number or of the trap geometry) translate directly into fluctuations of U_s . As will be discussed in more details in Section IV, these technical fluctuations add to the intrinsic relaxation due to quantum fluctuations and thereby play a significant role in the interpretation of the experiments.

We use a magnetic field \mathbf{B} aligned along the z axis to shift the energies of the individual Zeeman states $|m\rangle$, the eigenstates of \hat{s}_z with eigenvalues $m = 0, \pm 1$. Up to second order in B , the Zeeman Hamiltonian is $\hat{H}_Z = \sum_{i=1}^N p \hat{s}_{zi} + q \hat{s}_{zi}^2$, where $p \propto B$ and $q \propto B^2$ are the linear and quadratic Zeeman shifts, respectively. Noticing that $[\hat{S}_z, \hat{H}_{\text{int}}] = 0$, the first term in \hat{H}_Z is a constant of motion that can be removed by a unitary transformation. The total Hamiltonian thus reads [6]

$$\hat{H} = \hat{H}_{\text{int}} + \hat{H}_Z = \frac{U_s}{2N} \hat{\mathbf{S}}^2 + q (\hat{N}_{+1} + \hat{N}_{-1}), \quad (2)$$

where \hat{N}_m is the number of atoms in $|m\rangle$.

Under a mean-field approximation, the annihilation operators \hat{a}_m are replaced by the c -numbers $\sqrt{N} \zeta_m = \sqrt{N_m} \exp(i\phi_m)$. By convention we set $\phi_0 = 0$, and we focus on the situation $S_z = 0$. We define the mean number of $(+1, -1)$ pairs $N_p = (N_{+1} + N_{-1})/2$, and take its normalized value $n_p = N_p/N$ and the conjugate phase $\theta = \phi_{+1} + \phi_{-1}$ as dynamical variables. In terms of these variables, the mean-field equations of motion are [9]

$$\hbar \dot{n}_p = -2U_s n_p (1 - 2n_p) \sin \theta, \quad (3)$$

$$\hbar \dot{\theta} = -2q + 2U_s (4n_p - 1)(1 + \cos \theta). \quad (4)$$

At $t = 0$, the BEC is prepared in a generalized coherent spin state $|\psi_{\text{ini}}\rangle = (\sum_m \zeta_{\text{ini},m} |m\rangle)^{\otimes N}$, with

$$\zeta_{\text{ini}} = \begin{pmatrix} \sqrt{n_{\text{seed}}} e^{i \frac{\theta_{\text{ini}} + \eta_{\text{ini}}}{2}} \\ \sqrt{1 - 2n_{\text{seed}}} \\ \sqrt{n_{\text{seed}}} e^{i \frac{\theta_{\text{ini}} - \eta_{\text{ini}}}{2}} \end{pmatrix}, \quad (5)$$

where $n_{\text{seed}} = N_{\text{seed}}/N$ and N_{seed} is the number of atoms in the $m = \pm 1$ states. We then record the behavior of $N_p(t)$ as a function of time.

We notice that the state with all atoms in $m = 0$ (*i.e.* $N_{\text{seed}} = 0$ and hence $n_p = 0$) is stationary according to Eq. (3,4). However, this state is not an eigenstate of \hat{H}_{int} and thus not a stationary state of the quantum equation of motion. In the absence of a seed, we studied the resulting non-classical dynamics in [31] and identified two regimes:

- For $U_s/N \ll q$, the dynamics is reversible: The number of pairs $N_p(t)$ oscillates with a small amplitude.
- For $q \ll U_s/N$, the dynamics is strongly damped and $N_p(t)$ relaxes to a stationary value.

Here, we revisit these experiments to investigate the effect of a coherent seeding of the $m = \pm 1$ modes.

III. REVERSIBLE DYNAMICS

a. Theoretical predictions We focus first on the situation where $U_s/N \ll q \ll U_s$ and $n_{\text{seed}} \ll 1$. In this case, the reduced number of pairs n_p remains small at all times. Linearizing the mean-field Eqs. (3,4), we obtain [36]

$$N_p^{(\text{C})}(t) \approx \frac{2U_s}{q} \sin^2(\omega t) \cos^2\left(\frac{\theta_{\text{ini}}}{2}\right) N_{\text{seed}}, \quad (6)$$

where $\omega \approx \sqrt{2qU_s}$.

To improve the prediction (6) and account for quantum fluctuations, we use a semi-classical approach, the truncated Wigner approximation [2–5, 30]. The probability amplitudes $\zeta_{\text{ini},m}$ are treated as complex random variables which sample the initial Wigner distribution of the initial state at $t = 0$. The amplitudes are then propagated according to the mean-field equations of motion. Averaging the mean-field predictions over the fluctuations of ζ_{ini} , we find [30, 36]

$$N_p^{(\text{SC})}(t) \approx \frac{U_s}{2q} \sin^2(\omega t) \left[4 \cos^2\left(\frac{\theta_{\text{ini}}}{2}\right) N_{\text{seed}} + 1 \right]. \quad (7)$$

In analogy with quantum optics, the term $\propto N_{\text{seed}}$ in Eqs. (6,7) describes “stimulated emission” from the mode $m = 0$ to the modes $m = \pm 1$, while the additional term in Eq. (7) can be interpreted as “spontaneous emission”. We have verified numerically that the SC results are in good agreement with a fully quantum treatment. Moreover, comparing equations (6) and (7), we notice that unless the initial phase is chosen such that $\theta_{\text{ini}} \approx \pi$, a large seed $N_{\text{seed}} \gg 1$ makes the C and SC treatments almost identical, irrespective of the precise value of N . In fact, seeding with a few atoms $N_{\text{seed}} \approx 2 - 3$ and with $\theta = 0$ is sufficient to reach a 90 % agreement between the two approaches.

b. Experimental sequence We prepare a BEC in the state $m = 0$ using evaporative cooling in a crossed laser trap with a large magnetic field $B = 1$ G ($q \gg U_s$). After evaporation, the BEC contains $N \approx 2000$ atoms in the state $m = 0$, with $N_p \approx 100$ residual thermal atoms in $m = \pm 1$. We then turn on a strong magnetic field gradient to pull the $m = \pm 1$ atoms out of the trap. After this purification step, we measure $N_p \ll 1$ [27].

We add a coherent seed using a combination of magnetic field ramps and resonant radiofrequency (rf) pulses.

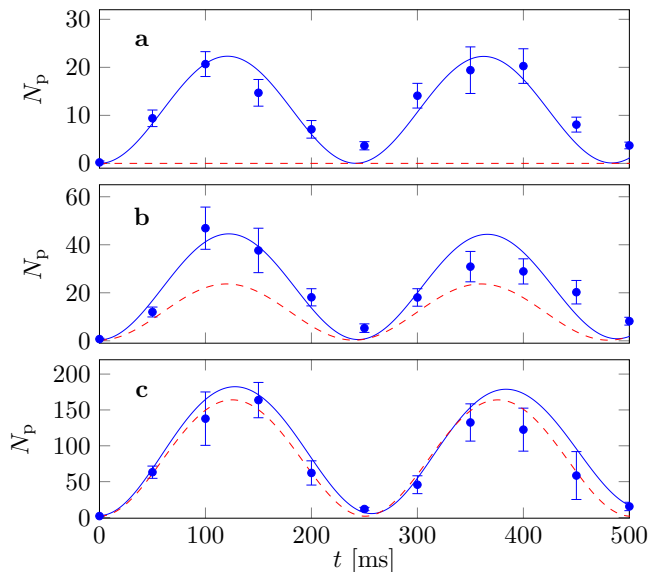


FIG. 1. Evolution of the number of $(+1, -1)$ pairs N_p (circles) for $q/h \approx 0.22 \pm 0.03$ Hz, $N \approx 1880 \pm 190$ atoms and various seed sizes: $N_{\text{seed}} \approx 0; 0.25; 1.8$ from (a) to (c). The initial phase is always set to $\theta_{\text{ini}} \approx 0$. The solid lines are numerical solutions of the Schrödinger equation using $U_s/h = 9.9$ Hz. The red dashed lines correspond to the classical prediction (6). Here and in the following, error bars show the statistical error corresponding to two standard errors.

For a proper choice of rf power and pulse duration, we are able to prepare any coherent spin state given by Eq. (5), up to the phase η_{ini} which is irrelevant for the experiments described here (see Supplementary Material [36] for more details). The main imperfection in the preparation originates from the fluctuations of the total atom number $\delta N \approx 0.1 N$, which induce $\approx 10\%$ relative fluctuations on N_{seed} . We then let the system evolve for a time t before measuring the population of each Zeeman state using a combination of Stern-Gerlach separation and fluorescence imaging with a detection sensitivity around 1.6 atoms per spin component [27].

c. Experimental results In Fig. 1, we show the time evolution of $N_p(t)$ for various initial states. In Fig. 1(a), we do not seed the dynamics. We observe an oscillation of $N_p(t)$, not captured by the classical description of Eq. (6), but in good agreement with the semi-classical predictions (7) or with the numerical resolution of the Schrödinger equation. In Fig. 1(b), we prepare a seed with $N_{\text{seed}} \approx 0.25 \pm 0.03$ (inferred from a calibration of the rf power) and $\theta_i \approx 0$. Compared to (a), the amplitude of the oscillations is doubled, in good agreement with (7). In Fig. 1(c), we set $N_{\text{seed}} \approx 1.8 \pm 0.2$ and $\theta_{\text{ini}} \approx 0$. The amplitude of the oscillations is further increased, and now also well reproduced by the fully classical treatment (6).

We investigate the role of the initial phase θ_{ini} in Fig. 2. In Fig. 2(a), we plot the variation of $N_p(T/2)$, with $T = \pi/(2\omega)$ the period of oscillations, against N_{seed} for three values of θ_{ini} . For $N_{\text{seed}} \ll 1$, we observe a

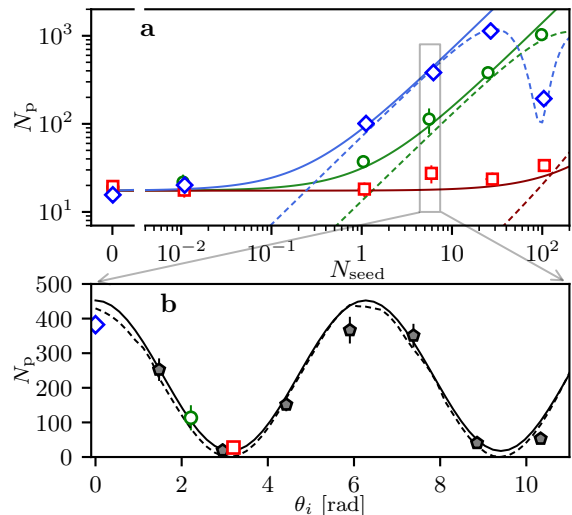


FIG. 2. (a) Number of pairs produced after half a period of evolution versus N_{seed} for $q/h \approx 0.33 \pm 0.03$ Hz and $N \approx 2920 \pm 280$. The blue diamonds, green circles and red squares correspond to initial phases $\theta_{\text{ini}} \approx 0; 2.2$; and 3.3 rad, respectively. For the three smallest seeds, N_{seed} is inferred from the calibration of the rf power. The solid lines are the semi-classical predictions given by Eq. (7) with $U_s/h \approx 12$ Hz. The dashed lines are the solutions of the classical mean-field Eqs. (3,4) with fixed initial conditions. (b) Scan of the initial phase θ_{ini} after half a period of evolution for $N_{\text{seed}} \approx 6.0$.

saturation of $N_p(T/2)$ at a value independent of θ_{ini} , consistent with the SC prediction (7). For such small seeds, the dynamics is triggered by quantum fluctuations. For larger seeds, unless the anti-phase-matching condition $\theta_{\text{ini}} \approx \pi$ is fulfilled, stimulated emission becomes dominant and the fully classical description is accurate. We observe a linear increase of $N_p(T/2)$ until the small-depletion approximation used to derive Eqs. (6,7) becomes inconsistent. For our data, this occurs for the point $N_{\text{seed}} \approx 100$, $\theta_{\text{ini}} \approx 0$. In this case, an exact resolution of the mean-field equations (3,4) provides accurate results. In Fig. 2(b), we set $N_{\text{seed}} \approx 6.0$ and scan the phase θ_{ini} . We measure oscillations of $N_p(T/2)$ in good agreement with Eqs. (6,7).

IV. RELAXATION DYNAMICS

a. Theoretical prediction We now investigate the relaxation dynamics in a very small magnetic field, such that $q \ll U_s/N$. In this regime, the quadratic Zeeman shift q is negligible and we set it to zero for the calculation. However, the assumption $n_p \ll 1$ used to derive Eq. (6) is not valid and the mean-field equations (3,4) cannot be linearized. We are nevertheless able to directly solve these equations. Taking for simplicity $\theta_{\text{ini}} = 0$, we

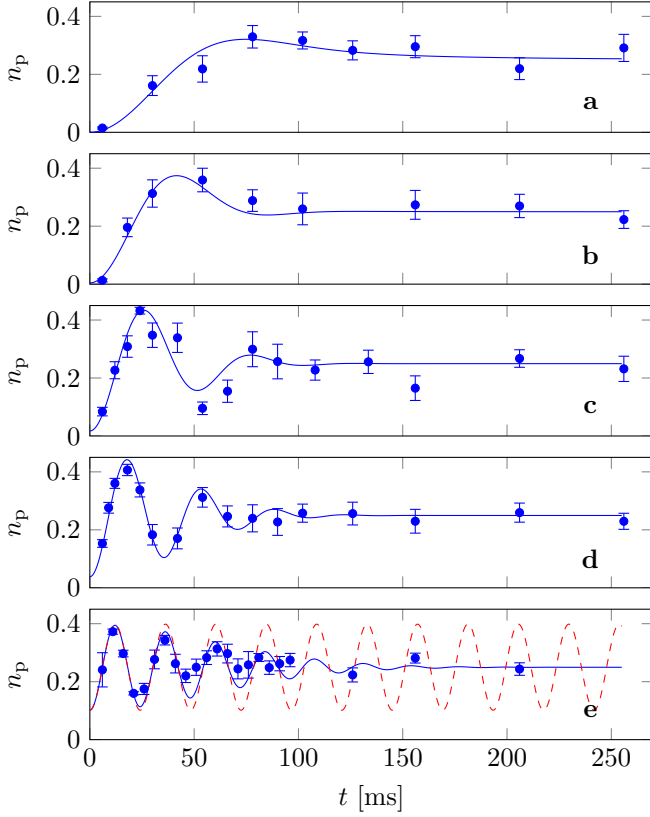


FIG. 3. Evolution of the fraction of $(+1, -1)$ pairs $n_p = N_p/N$ in a negligible magnetic field, for $N \approx 124 \pm 12$ atoms and various seedings: $N_{\text{seed}} = 0; 0.54; 2.1; 4.9; 12.8$; from (a) to (e). The initial phase is always set to $\theta_{\text{ini}} \approx 0$. The solid lines are numerical solutions of the Schrödinger equation for $U_s/h = 24.5$ Hz. In (e), the red dashed line is the classical prediction from Eqs.(3,4).

find [36]

$$n_p^{(C)}(t) = \frac{1}{4} - \frac{1 - 4n_{\text{seed}}}{4} \cos(\Omega t), \quad (8)$$

with an oscillation frequency

$$\Omega = \frac{4U_s}{\hbar} \sqrt{2n_{\text{seed}}(1 - 2n_{\text{seed}})}. \quad (9)$$

The non-linear dependence of Ω with n_{seed} reflects the non-linearity of the mean-field equations, and has dramatic consequences when one takes into account quantum fluctuations. The seeds spontaneously created from the vacuum of pairs induce random shifts of the oscillation frequency around its mean-field value. Averaging over many realizations therefore results in an intrinsic dephasing of the oscillations predicted in Eq.(8). More precisely, for the generalized coherent spin state prepared in our experiment, the initial number of atoms in the $m = \pm 1$ modes $N_{+1,\text{ini}} + N_{-1,\text{ini}} = \Sigma$ follows a binomial distribution of mean $2N_{\text{seed}}$ (quantum partition noise). We use the random variable Σ as an initial condition

to solve the mean-field equations (3,4), *i.e.* substituting n_{seed} in Eq.(8) with $\Sigma/(2N)$. After averaging over the partition noise, we obtain for $N_{\text{seed}} \gg 1$ [36]

$$n_p^{(\text{SC})}(t) \approx \frac{1}{4} - \frac{1 - 4n_{\text{seed}}}{4} \cos(\Omega t) e^{-\frac{1}{2}(\gamma_c t)^2}, \quad (10)$$

with a collapse rate

$$\gamma_c = \frac{2U_s}{\sqrt{N}\hbar} |1 - 4n_{\text{seed}}|. \quad (11)$$

The analytic formula (10) agrees very well with the numerical solution of the many-body Schrödinger equation for $N_{\text{seed}} \gtrsim 1$.

In an actual experiment, the relaxation of N_p is also enhanced by purely classical noise sources of technical origin. In our case, we identify shot-to-shot fluctuations of U_s (see Section II) as a significant additional mechanism contributing to the blurring of the oscillations. To account for this phenomenon, we average Eq.(10) over a Gaussian distribution of U_s with variance δU_s^2 . The resulting $n_p(t)$ has the same functional form as in Eq.(10) with the replacement

$$\gamma_c \rightarrow \Gamma = \sqrt{\gamma_c^2 + \gamma_t^2}, \quad (12)$$

with a technical blurring rate

$$\gamma_t = \frac{4\delta U_s}{\hbar} \sqrt{2n_{\text{seed}}(1 - 2n_{\text{seed}})}. \quad (13)$$

For small enough seeds $n_{\text{seed}} \ll 1/4$, the total dephasing rate can be written

$$\Gamma \approx \gamma_c \sqrt{1 + 2 \left(\frac{2\delta U_s}{U_s} \right)^2 N_{\text{seed}}}. \quad (14)$$

This indicates a crossover from quantum to classical dephasing for seed sizes $N^* \approx U_s^2/(2\delta U_s)^2$.

b. Experimental considerations In order to achieve the “zero field” regime $Nq \ll U_s$ experimentally, the best option is to reduce the atom number. Indeed, increasing the trap confinement and U_s also increases undesired inelastic processes. Reducing the applied magnetic field further is not feasible due to ambient stray fields and environment-induced fluctuations (at the sub-mG level in our experiment). Reducing N is also more favorable to achieve the regime $\gamma_c \gg \gamma_t$ and observe the quantum collapse of the dynamics, given the scaling $\gamma_c \propto 1/\sqrt{N}$. We therefore prepare mesoscopic BECs of $N \approx 124 \pm 12$ atoms in the same initial spin state as before, but in a tighter trap in order to achieve $U_s/h \approx 24.5$ Hz (more details in the Supplementary Material).

c. Experimental results We show in figure 3 the relaxation dynamics of n_p for various seed sizes n_{seed} . We observe an acceleration of the initial dynamics for increasing n_{seed} and the emergence of rapidly damped oscillations. Eventually, n_p relaxes to the stationary value $\approx 1/4$ in all cases. Numerical simulations with U_s taken

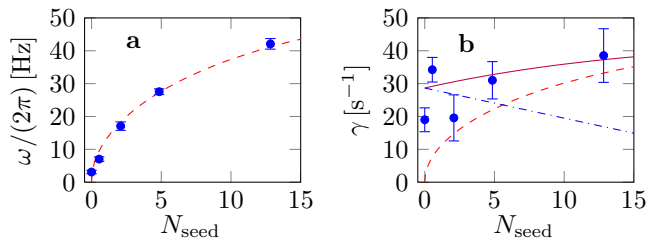


FIG. 4. Frequency (a) and relaxation rate (b) of the spin-mixing dynamics in a negligible magnetic field. The circles are obtained from a fit to the data of Fig. 3, with the error bars indicating the 95% confidence interval. In (a), the red dashed line corresponds to the frequency ω predicted by the mean-field treatment. In (b), the dash-dotted blue line corresponds to the rate γ_c of the collapse driven by quantum fluctuations, the red dashed line is the damping rate γ_t due to technical fluctuations, and the solid purple line corresponds to the total damping rate $\Gamma = [\gamma_c^2 + \gamma_t^2]^{1/2}$. We use the value $\delta U_s/U_s = 0.13 \pm 0.04$, obtained from a fit to the data.

as a fit parameter are overall in good agreement with the data, although they slightly underestimate the damping rate for the largest seed $N_{\text{seed}} = 12.8$.

To compare these experiments with the theoretical predictions, we fit a function of the form (10) to the data of Fig. 3, leaving Ω and Γ as free parameters. We report in Fig. 4a,b the fitted frequency and relaxation rate. The frequency is essentially insensitive to quantum or classical fluctuations, and the measured values agree well with the C or SC predictions. The relaxation rate varies little with N_{seed} in the range we have explored experimentally. This observation is explained by the SC theory including technical fluctuations. Indeed, the slow decrease of γ_c with N_{seed} is compensated by the increase of γ_t . Using $\delta U_s/U_s \approx 0.13$ as determined in Fig. (4), we find a “quantum-classical crossover” for seed sizes around $N^* \approx 14.8$, close to the largest value we explored experimentally. For small seeds $N_{\text{seed}} \lesssim 5$, our measurements are consistent with a collapse driven primarily by

quantum fluctuations. On the contrary, for the largest $N_{\text{seed}} \approx 12.8$, classical technical dephasing is the dominant damping mechanism.

V. CONCLUSION

We investigated the dynamics of a spin-1 BEC prepared with a majority of atoms in the Zeeman state $m = 0$ and possibly small coherent seeds in the $m = \pm 1$ modes. For a small but non-negligible magnetic field, we observe oscillations of the spin populations. This dynamics is triggered by quantum fluctuations in the absence of a seed, and cannot be captured in a completely classical approach. Adding a coherent seed is phase-sensitive [30]. In general it corresponds to a dramatic increase of the oscillation amplitude, and the classical predictions become accurate as soon as a few atoms (typically $N_{\text{seed}} \gtrsim 2$) are used to seed the dynamics.

We also studied the dynamics in a negligible magnetic field. In this second regime, the combination of non-linear mean-field equations and quantum noise leads to the relaxation of the spin populations. When the size of the seed increases, the intrinsic damping rate γ_c decreases and the mean-field picture becomes more and more relevant. However, it eventually fails for sufficiently long times. Experimentally, technical noise sources provide additional dephasing mechanisms of purely classical origin that can be completely described in the mean-field approach. In our experiment, we identify the fluctuations of the total atom number as the leading blurring mechanism when the seed size exceeds a dozen atoms.

All the experiments presented in this Letter are well captured by a semi-classical theory, where quantum fluctuations are modeled using stochastic classical variables. An interesting direction for future work would be to test experimentally the validity of such a semi-classical description in other contexts, in particular in a chaotic regime [31, 37, 38].

-
- [1] C. Gardiner and P. Zoller, *Quantum noise* (Springer Science, 2004).
 - [2] A. Polkovnikov, *Annals of Physics* **325**, 1790 (2010).
 - [3] M. J. Steel, M. K. Olsen, L. I. Plimak, P. D. Drummond, S. M. Tan, M. J. Collett, D. F. Walls, and R. Graham, *Phys. Rev. A* **58**, 4824 (1998).
 - [4] A. Sinatra, C. Lobo, and Y. Castin, *Journal of Physics B: Atomic, Molecular and Optical Physics* **35**, 3599 (2002).
 - [5] R. Mathew and E. Tiesinga, *Phys. Rev. A* **96**, 013604 (2017).
 - [6] Y. Kawaguchi and M. Ueda, *Physics Reports* **520**, 253 (2012).
 - [7] W. Zhang, S. Yi, and L. You, *New Journal of Physics* **5**, 77 (2003).
 - [8] D. Jacob, L. Shao, V. Corre, T. Zibold, L. De Sarlo, E. Mimoun, J. Dalibard, and F. Gerbier, *Phys. Rev. A* **86**, 061601 (2012).
 - [9] W. Zhang, D. L. Zhou, M.-S. Chang, M. S. Chapman, and L. You, *Phys. Rev. A* **72**, 013602 (2005).
 - [10] M.-S. Chang, Q. Qin, W. Zhang, L. You, and M. S. Chapman, *Nature Physics* **1**, 111 (2005).
 - [11] J. Kronjäger, C. Becker, M. Brinkmann, R. Walser, P. Navez, K. Bongs, and K. Sengstock, *Phys. Rev. A* **72**, 063619 (2005).
 - [12] J. Kronjäger, C. Becker, P. Navez, K. Bongs, and K. Sengstock, *Phys. Rev. Lett.* **97**, 110404 (2006).
 - [13] A. T. Black, E. Gomez, L. D. Turner, S. Jung, and P. D. Lett, *Phys. Rev. Lett.* **99**, 070403 (2007).
 - [14] Y. Liu, E. Gomez, S. E. Maxwell, L. D. Turner, E. Tiesinga, and P. D. Lett, *Phys. Rev. Lett.* **102**, 225301 (2009).
 - [15] C. Klempt, G. Gebreyesus, M. Scherer, T. Henninger,

- P. Hyllus, W. Ertmer, L. Santos, and J. J. Arlt, Phys. Rev. Lett. **104**, 195303 (2010).
- [16] E. M. Bookjans, C. D. Hamley, and M. S. Chapman, Phys. Rev. Lett. **107**, 210406 (2011).
- [17] B. Lücke, M. Scherer, J. Kruse, L. Pezze, F. Deuretzbacher, P. Hyllus, J. Peise, W. Ertmer, J. Arlt, L. Santos, et al., Science **334**, 773 (2011).
- [18] C. D. Hamley, C. Gerving, T. Hoang, E. Bookjans, and M. S. Chapman, Nat. Phys. **8**, 305 (2012).
- [19] B. Lücke, J. Peise, G. Vitagliano, J. Arlt, L. Santos, G. Tóth, and C. Klempt, Phys. Rev. Lett. **112**, 155304 (2014).
- [20] D. Linnemann, H. Strobel, W. Muessel, J. Schulz, R. J. Lewis-Swan, K. V. Kheruntsyan, and M. K. Oberthaler, Phys. Rev. Lett. **117**, 013001 (2016).
- [21] D. Linnemann, J. Schulz, W. Muessel, P. Kunkel, M. Prüfer, A. Frölian, H. Strobel, and M. Oberthaler, Quantum Science and Technology **2**, 044009 (2017).
- [22] P. Kunkel, M. Prüfer, H. Strobel, D. Linnemann, A. Frölian, T. Gasenzer, M. Gärttner, and M. K. Oberthaler, Science **360**, 413 (2018).
- [23] M. Fadel, T. Zibold, B. Décamps, and P. Treutlein, Science **360**, 409 (2018).
- [24] K. Lange, J. Peise, B. Lücke, I. Kruse, G. Vitagliano, I. Apellaniz, M. Kleinmann, G. Tóth, and C. Klempt, Science **360**, 416 (2018).
- [25] T. Tian, H.-X. Yang, L.-Y. Qiu, H.-Y. Liang, Y.-B. Yang, Y. Xu, and L.-M. Duan, Phys. Rev. Lett. **124**, 043001 (2020).
- [26] H.-X. Yang, T. Tian, Y.-B. Yang, L.-Y. Qiu, H.-Y. Liang, A.-J. Chu, C. B. Dag, Y. Xu, Y. Liu, and L.-M. Duan, Phys. Rev. A **100**, 013622 (2019).
- [27] A. Qu, B. Evrard, J. Dalibard, and F. Gerbier, Phys. Rev. Lett. **125**, 033401 (2020).
- [28] G. I. Mias, N. R. Cooper, and S. Girvin, Phys. Rev. A **77**, 023616 (2008).
- [29] X. Cui, Y. Wang, and F. Zhou, Phys. Rev. A **78**, 050701 (2008).
- [30] J. P. Wrubel, A. Schwettmann, D. P. Fahey, Z. Glassman, H. Pechkis, P. Griffin, R. Barnett, E. Tiesinga, and P. Lett, Phys. Rev. A **98**, 023620 (2018).
- [31] B. Evrard, A. Qu, J. Dalibard, and F. Gerbier, Arxiv (2020), 2010.13832.
- [32] S. Yi, Ö. Müstecaplıoğlu, C.-P. Sun, and L. You, Phys. Rev. A **66**, 011601 (2002).
- [33] T. Ohmi and K. Machida, Journal of the Physical Society of Japan **67**, 1822 (1998).
- [34] T.-L. Ho, Phys. Rev. Lett. **81**, 742 (1998).
- [35] F. Dalfovo, S. Giorgini, L. P. Pitaevskii, and S. Stringari, Reviews of Modern Physics **71**, 463 (1999).
- [36] for more details see Supplemental Material, which includes the reference [39].
- [37] M. Rautenberg and M. Gärttner, Phys. Rev. A **101**, 053604 (2020).
- [38] J. Tomkovič, W. Muessel, H. Strobel, S. Löck, P. Schlagheck, R. Ketzmerick, and M. K. Oberthaler, Phys. Rev. A **95**, 011602 (2017).
- [39] S. Uchino, M. Kobayashi, and M. Ueda, Phys. Rev. A **81**, 063632 (2010).

Supplemental Material: Coherent seeding of the dynamics of a spinor Bose-Einstein condensate: from quantum to classical behavior

VI. INITIAL STATE PREPARATION

A. Oscillating regime

We prepare the spinor BEC at $t = 0$ in a generalized coherent spin state $|\psi_{\text{ini}}\rangle = (\sum_m \zeta_{\text{ini},m} |m\rangle)^{\otimes N}$,

$$\zeta_{\text{ini}} = \begin{pmatrix} \sqrt{n_{\text{seed}}} e^{i\frac{\theta_{\text{ini}} + \eta_{\text{ini}}}{2}} \\ \sqrt{1 - 2n_{\text{seed}}} \\ \sqrt{n_{\text{seed}}} e^{i\frac{\theta_{\text{ini}} - \eta_{\text{ini}}}{2}} \end{pmatrix}. \quad (\text{S1})$$

We prepare this state starting from $|m = 0\rangle$ using a combination of magnetic field ramps and resonant radio-frequency (rf) pulses. In details, we first pulse a rf field resonant with the Zeeman splitting to populate the $m = \pm 1$ modes with a fraction $n_{\text{seed}} = \sin^2(\Omega_{\text{rf}} t_1)/2$ of the atoms. Here, Ω_{rf} is the rf Rabi frequency and t_1 the pulse duration. At this stage, we have prepared a coherent spin state of the form (S1) with $\theta_{\text{ini}} \approx \pi$.

To change θ_{ini} , we let the system evolve in a field $B = 0.5 \text{ G}$ ($q/h \approx 70 \text{ Hz}$) for a time $t_2 < h/(2q)$, before quenching the magnetic field down to $28 \pm 2 \text{ mG}$ ($q/h \approx 0.22 \text{ Hz}$) in $t_3 = 4 \text{ ms}$ to achieve the desired regime $U_s/N \ll q \ll U_s$. Interactions are negligible ($U_s/h \approx 10 \text{ Hz}$ hence $U_s t_{2,3}/h \ll 1$), and the system simply acquires a phase shift $\Delta\theta_2 = -2qt_2/h$ while the magnetic field is held constant, and $\Delta\theta_3 = -2 \int q(t)dt/h$ during the quench. This results in an initial phase $\theta_{\text{ini}} = \pi - 2qt_2/h + \Delta\theta_3$ that is fully tunable from 0 to 2π by varying t_2 .

B. Relaxing regime

We prepare mesoscopic BECs of $N \approx 124$ atoms in the same initial spin state as before. We lower the magnetic field down to $B = 4.2 \pm 1.5 \text{ mG}$ ($q/h \approx 5 \text{ mHz}$) in $t_3 = 20 \text{ ms}$. The ramp time corresponds to the time needed for the damping of eddy currents in the vacuum chamber. Because of the small atom number, the effects of the spin dependent interactions are negligible over the ramp ($U_s/h \approx 4 \text{ Hz}$, such that $U_s t_3/h \ll 1$) and the evolution of the state is essentially another phase shift of θ , which can be compensated for by varying t_2 . For these experiments, we always choose t_2 such that $\theta_{\text{ini}} \approx 0$.

Finally, we trigger the dynamics by recompressing the trap in 6 ms ($U_s/h \approx 4 \rightarrow 24 \text{ Hz}$). By performing numerical simulations of the sequence with the many-body Schrödinger equation, we have checked that the ramp can be considered instantaneous to a good approximation.

VII. CLASSICAL AND SEMI-CLASSICAL DYNAMICS

We detail here the calculations of the dynamics of $N_p(t)$ given in the main text. We use a classical (C) approach based on the mean-field approximation and a semi-classical (SC) approach inspired by the truncated Wigner approximation (TWA). In both frameworks, the annihilation operators \hat{a}_m are replaced by c -numbers $\alpha_m = \sqrt{N}\zeta_m$, with N the number of condensed atoms and ζ a spin-1 wavefunction (normalized to unity) parameterized as

$$\zeta = \begin{pmatrix} \sqrt{n_p} e^{i\frac{\theta + \eta}{2}} \\ \sqrt{1 - 2n_p} \\ \sqrt{n_p} e^{i\frac{\theta - \eta}{2}} \end{pmatrix}. \quad (\text{S2})$$

Here $n_p = (N_{+1} + N_{-1})/(2N)$ denotes the average number of $m = \pm 1$ pair normalized to the total atom number ($N_p = Nn_p$), and we have restricted ourselves to the situation $N_{+1} = N_{-1}$. We also have chosen ζ_0 real without loss of generality.

The mean field equations of motion for a spin-1 condensate in the single-mode regime take the form [1, 2]

$$\hbar \dot{n}_p = -2U_s n_p (1 - 2n_p) \sin \theta \quad (\text{S3})$$

$$\hbar \dot{\theta} = -2q + 2U_s (4n_p - 1)(1 + \cos \theta). \quad (\text{S4})$$

The mean-field energy per atom is given by

$$\mathcal{E}_s = 2U_s n_p (1 - 2n_p)(1 + \cos \theta) + 2qn_p. \quad (\text{S5})$$

The energy \mathcal{E}_s is a constant of motion, a fact that we will use repeatedly in the following.

A. Dynamics in the oscillating regime

In this section we derive the evolution of $N_p(t)$ for the oscillating regime $q \gg U_s/N$. We assume $N_{\text{seed}} \ll N$, i.e. the situation where quantum fluctuations may play a significant role. For $N_{\text{seed}} \sim N$, a fully classical treatment is accurate.

a. Classical solution : Assuming $n_p \ll 1$, we linearize Eqs. (S3) and (S5),

$$\hbar \dot{n}_p \approx -2U_s n_p \sin \theta \quad (\text{S6})$$

$$\mathcal{E}_s \approx (2U_s(1 + \cos \theta) + 2q)n_p. \quad (\text{S7})$$

We use the second equation to express $\cos \theta$ as a function of n_p and of the constants q, U_s, \mathcal{E}_s . Substituting in the first equation, we obtain a differential equation on n_p only, $\dot{n}_p^2 = -4\omega^2 [n_p - \alpha]^2 + A$, where

$$\hbar\omega = \sqrt{q(q + 2U_s)}, \quad \alpha = \frac{\mathcal{E}_s(q + U_s)}{2(\hbar\omega)^2}, \quad (\text{S8})$$

and where A is constant. Differentiating one more time, we find that either n_p is constant or it obeys the harmonic equation $\ddot{n}_p + 4\omega^2(n_p - \alpha) = 0$. The evolution is thus a harmonic motion at frequency 2ω ,

$$n_p(t) \approx n_{\text{seed}} + 2(\alpha - n_{\text{seed}}) \sin^2(\omega t), \quad (\text{S9})$$

with the initial conditions $n_p(0) = n_{\text{seed}}$ and $\theta(0) = \theta_{\text{ini}}$.

If we also assume (as in the experiments we performed) that $q \ll U_s$, we have $\mathcal{E}_s \approx 4U_s n_{\text{seed}} \cos^2(\theta_{\text{ini}}/2) \gg q$, and $\alpha \approx \mathcal{E}_s/(4q) \gg 1$. Eq. (S9) then reduces to

$$n_p(t) \approx n_{\text{seed}} + \frac{2U_s n_{\text{seed}}}{q} \cos^2(\theta_{\text{ini}}/2) \sin^2(\omega t),$$

i.e. to Eq. (6) in the main text.

b. Semi-classical picture : We now consider the effect of quantum fluctuations within the TWA [3–7]. In this method, the c -numbers α_m used instead of the annihilation operators \hat{a}_m in the mean-field approximation are treated as complex random variables. At $t = 0$, these variables sample the Wigner distribution of the initial state $|\psi_i\rangle$. Their mean values are given by

$$\bar{\alpha}_{\text{ini}} = N \begin{pmatrix} \sqrt{n_{\text{seed}}} e^{i\frac{\theta_{\text{ini}} + \eta_{\text{ini}}}{2}} \\ \sqrt{1 - 2n_{\text{seed}}} \\ \sqrt{n_{\text{seed}}} e^{i\frac{\theta_{\text{ini}} - \eta_{\text{ini}}}{2}} \end{pmatrix}. \quad (\text{S10})$$

In the limit $N_{\text{seed}} \ll N$, the calculation can be simplified by neglecting the depletion of the mode $m = 0$. For the $m = \pm 1$ modes, this approximation amounts to replacing coherent spin states by harmonic oscillator coherent states, which are considerably easier to handle. The initial quantum state is thus taken to be

$$|\psi_{\text{ini}}\rangle \approx \frac{1}{\sqrt{N!}} \prod_{m=\pm 1} e^{\bar{\alpha}_{m,\text{ini}} \hat{a}_m^\dagger - \bar{\alpha}_{m,\text{ini}}^* \hat{a}_m} \hat{a}_0^{\dagger N} |\text{vac}\rangle. \quad (\text{S11})$$

For $t > 0$, the equations of evolution (S3,S4) remain valid in the TWA. The solution for initial conditions $\alpha_{\pm 1,\text{ini}}$ is thus given by Eq. (S9) with the substitution $4N_{\text{seed}} \cos^2(\theta_{\text{ini}}/2) \rightarrow |\alpha_{+1,\text{ini}} + \alpha_{-1,\text{ini}}^*|^2$.

To average over the initial distribution of $\alpha_{\pm 1,\text{ini}}$, we recall that the Wigner distribution average $\langle \mathcal{O}(\alpha_m, \alpha_m^*) \rangle_{\text{Wig}}$ of an operator \mathcal{O} is equal to the expectation value $\langle \mathcal{O}^{\text{sym}}(\hat{a}_m, \hat{a}_m^\dagger) \rangle$ of the corresponding symmetrically ordered operator \mathcal{O}^{sym} [3]. We obtain

$$\langle \alpha_{+1,\text{ini}} \alpha_{-1,\text{ini}}^* \rangle_{\text{Wig}} = \langle \hat{a}_{+1} \hat{a}_{-1}^\dagger \rangle = \bar{\alpha}_{+1,\text{ini}} \bar{\alpha}_{-1,\text{ini}}^*, \quad (\text{S12})$$

$$\langle |\alpha_{m,\text{ini}}|^2 \rangle_{\text{Wig}} = \frac{1}{2} \langle \hat{a}_m^\dagger \hat{a}_m + \hat{a}_m \hat{a}_m^\dagger \rangle = |\bar{\alpha}_{m,\text{ini}}|^2 + \frac{1}{2}. \quad (\text{S13})$$

This leads to

$$\langle N_p(t) \rangle \approx \frac{U_s}{2q} \sin^2(\omega t) (|\bar{\alpha}_{+1,\text{ini}} + \bar{\alpha}_{-1,\text{ini}}^*|^2 + 1),$$

which gives Eq. (7) in the main text.

As a final remark, we note that the Bogoliubov method is also well suited to study the regime that we investigated here, and leads to the same result [8–10].

B. Relaxation dynamics

We now discuss the regime $q \ll U_s/N$, in which we observe a relaxation of the number of pairs N_p to a stationary value. In this regime, the quantum fluctuations play an important role even for $N_{\text{seed}} \gg 1$. We will thus consider that $N_{\text{seed}} \gg 1$ and $N - N_{\text{seed}} \gg 1$. For simplicity, we will focus on the situation $\theta_{\text{ini}} = 0$, for which the effect of the seed is maximal. The case with no seed has been treated using an exact diagonalization of the Hamiltonian [10] or the TWA [6].

a. Classical solution In order to simplify the calculation, we neglect completely the quadratic Zeeman shift. In this regime $q \ll U_s/N$, the Zeeman term indeed plays no significant role even for the fully quantum model. Introducing the auxiliary variable $x = 4n_p - 1$, the equations of motion and the energy become

$$\hbar \dot{x} = -U_s(1 - x^2) \sin \theta, \quad (\text{S14})$$

$$\hbar \dot{\theta} = 2U_s x(1 + \cos \theta), \quad (\text{S15})$$

$$\mathcal{E}_s = \frac{U_s}{4}(1 - x^2)(1 + \cos \theta) = \text{cst}. \quad (\text{S16})$$

We combine the first and last equations to obtain

$$\dot{x} = -\frac{4\mathcal{E}_s}{\hbar} \frac{\sin \theta}{1 + \cos \theta}. \quad (\text{S17})$$

Differentiating this equation, we eliminate the phase θ and obtain a simple harmonic equation, $\ddot{x} = -\Omega^2 x$, with an oscillation frequency $\hbar\Omega = \sqrt{8U_s \mathcal{E}_s}$. For the initial conditions $n_p(0) = n_{\text{seed}}$ and $\theta(0) = 0$, we have $\hbar\Omega = 2U_s \sqrt{1 - x_0^2}$ and $x(t) = x_0 \cos(\Omega t)$ with $x_0 = 4n_{\text{seed}} - 1$. This corresponds to the results announce in Eqs. (8,9) of the main text.

b. Quantum partition noise: The initial state

$$|\psi_{\text{ini}}\rangle = \frac{1}{\sqrt{N!}} \left[\sum_{m=0,\pm 1} \zeta_m \hat{a}_m^\dagger \right]^N |\text{vac}\rangle,$$

is characterized by fluctuations of the number of ± 1 atoms. We consider again the states with $|\zeta_{+1}| = |\zeta_{-1}| = \sqrt{N_{\text{seed}}}$ and $\theta_i = 0$. We introduce the sum $\Sigma = N_{+1} + N_{-1}$, its relative value $s = \Sigma/N$ and the difference $\Delta = N_{+1} - N_{-1}$. The components of ζ are related to the average $\bar{\Sigma}$ of Σ by

$$|\zeta_{\pm 1}|^2 = \frac{\bar{\Sigma}}{2}, \quad |\zeta_0|^2 = N - \bar{\Sigma}. \quad (\text{S18})$$

The joint distribution of Σ and Δ in the initial coherent spin state is

$$\mathcal{P}(\Sigma, \Delta) = \frac{N!}{\left(\frac{\Sigma+\Delta}{2}\right)! \left(\frac{\Sigma-\Delta}{2}\right)! (N-\Sigma)!} \left(\frac{\bar{s}}{2}\right)^\Sigma (1 - \bar{s})^{N-\Sigma}. \quad (\text{S19})$$

We deduce from Eq. (S19) the distribution of Σ ,

$$\mathcal{P}(\Sigma) = \frac{N!}{\Sigma! (N-\Sigma)!} \bar{s}^\Sigma (1 - \bar{s})^{N-\Sigma}. \quad (\text{S20})$$

with $\Sigma \in [0, N]$. The normalization follows from the binomial formula.

For large N and Σ away from the extreme values $0, N$, the binomial distribution is well approximated by a continuous Gaussian distribution

$$\mathcal{P}(\Sigma) \approx \frac{1}{N} \frac{1}{\sqrt{2\pi}\sigma} e^{-\frac{(\Sigma-\bar{s})^2}{2\sigma^2}} = p(s)ds. \quad (\text{S21})$$

with a step size $ds = 1/N$ and a standard deviation

$$\sigma = \sqrt{\frac{\bar{s}(1-\bar{s})}{N}} = \sqrt{\frac{2n_{\text{seed}}(1-2n_{\text{seed}})}{N}}. \quad (\text{S22})$$

One can check the normalization of both distributions,

$$\sum_{\Sigma=0}^N \mathcal{P}(\Sigma) \rightarrow \int_0^1 f(s)ds \approx \int_{-\infty}^{+\infty} \frac{1}{\sqrt{2\pi}} e^{-\frac{u^2}{2}} du = 1.$$

To extend the lower boundary to $-\infty$, we require $\bar{s}/\sigma = \sqrt{N} \times \sqrt{\bar{s}/(1-\bar{s})} \gg 1$, or $N\bar{s} = 2N_{\text{seed}} \gg 1$.

c. Semi-classical picture of the dynamics: Similarly to what we have done in Sec. VII A, we average the mean field solution (S3,S4) with $2n_{\text{seed}} \rightarrow s$ over the probability distribution $p(s)$ in Eq. (S21). This amounts to compute the integral

$$I = \frac{1}{2} \int_0^1 s \cos[\Omega(s)t] p(s) ds. \quad (\text{S23})$$

We use the fact that $p(s)$ is sharply peaked around \bar{s} , with a width $\sim 1/N$ much narrower than the scale of variation of the rest of the integrand $s \cos[\Omega(s)t]$. As a result, we extend the integral boundaries to $\pm\infty$, set $s \approx \bar{s}$ and expand the frequency $\Omega(s)$ to first order,

$$\Omega(s) \approx \bar{\Omega} + \bar{\Omega}'(s - \bar{s}) + \mathcal{O}(\epsilon^2), \quad (\text{S24})$$

where $\bar{\Omega} = \Omega(\bar{s})$ and $\bar{\Omega}' = \Omega'(\bar{s}) = (2U_s/\hbar) \times (1 - 2\bar{s})/\sqrt{\bar{s}(1-\bar{s})}$.

With straightforward manipulations, we cast I in the form of the Fourier transform of a Gaussian function, which is readily calculated. We find

$$I = \frac{1}{2} \bar{s} \cos[\bar{\Omega}t] e^{-\frac{1}{2}(\gamma_c t)^2}, \quad (\text{S25})$$

with a damping rate

$$\gamma_c = |\bar{\Omega}'\sigma| = \frac{2U_s}{\sqrt{N}\hbar} |1 - 2\bar{s}|. \quad (\text{S26})$$

Using $\bar{s} = 2n_{\text{seed}}$, this gives Eq. (11) in the main text.

d. Classical fluctuations of Ω : In addition to the intrinsic dephasing originating from quantum fluctuations, any technical fluctuations of Ω will also contribute to the observed relaxation. We consider here the dominant source of classical blurring in our experiment, namely fluctuations of the interaction strength U_s mainly due to shot-to-shot atom number fluctuations.

We model these fluctuations by considering a fluctuating interaction strength $U'_s = U_s + \delta U_s x$, with U_s the average value, δU_s the standard deviation of the noise, and x a centered Gaussian random variable of variance unity. This leads to a fluctuating oscillation frequency $\Omega(x) = \bar{\Omega}(1 + x \cdot \delta U_s/U_s)$. We neglect the fluctuations of γ_c , which is legitimate for $N_{\text{seed}} \gg 1$ and hence $\gamma_c \ll \bar{\Omega}$. Averaging over the Gaussian probability distribution $p(x)$, we find that

$$I_2 = \left\langle \cos[\Omega(x)t] e^{-\frac{1}{2}(\gamma_c t)^2} \right\rangle_x = \cos[\bar{\Omega}t] e^{-\frac{1}{2}(\gamma_t t)^2 - \frac{1}{2}(\gamma_c t)^2}, \quad (\text{S27})$$

with a classical (technical) damping rate given by

$$\gamma_t = \bar{\Omega} \frac{\delta U_s}{U_s}. \quad (\text{S28})$$

From Eqs. (S27,S28) we obtain Eqs. (12,13) given in the main text.

-
- [1] W. Zhang, D. L. Zhou, M.-S. Chang, M. S. Chapman, and L. You, Phys. Rev. A **72**, 013602 (2005).
 - [2] Y. Kawaguchi and M. Ueda, Physics Reports **520**, 253 (2012).
 - [3] A. Polkovnikov, Annals of Physics **325**, 1790 (2010).
 - [4] M. J. Steel, M. K. Olsen, L. I. Plimak, P. D. Drummond, S. M. Tan, M. J. Collett, D. F. Walls, and R. Graham, Phys. Rev. A **58**, 4824 (1998).
 - [5] A. Sinatra, C. Lobo, and Y. Castin, Journal of Physics B: Atomic, Molecular and Optical Physics **35**, 3599 (2002).
 - [6] R. Mathew and E. Tiesinga, Phys. Rev. A **96**, 013604 (2017).

- [7] J. P. Wrubel, A. Schwettmann, D. P. Fahey, Z. Glassman, H. Pechkis, P. Griffin, R. Barnett, E. Tiesinga, and P. Lett, Phys. Rev. A **98**, 023620 (2018).
- [8] G. I. Mias, N. R. Cooper, and S. Girvin, Phys. Rev. A **77**, 023616 (2008).
- [9] S. Uchino, M. Kobayashi, and M. Ueda, Phys. Rev. A **81**, 063632 (2010).
- [10] B. Evrard, A. Qu, J. Dalibard, and F. Gerbier, Arxiv (2020), 2010.13832.